Atomization and Sprays, vol. 8, pp. 503-519, 1998

EFFECT OF COAL PARTICLE SIZE ON COAL-WATER SLURRY (CWS) ATOMIZATION

S. Y. Son and K. D. Kihm
Department of Mechanical Engineering, Texas A&M University, College Station, Texas, U.S.A.

To determine the effect of coal particle size on coal-water slurry (CWS) atomization, Sauter mean diameters (SMD) of spray droplets have been measured for various slurries containing three different coal particle sizes (32-45 μm, 45-63 μm, and 63-90 μm). The test sprays are generated by a sonic air jet blasting onto the cross-injecting CWS mixture. The diffraction particle analyzing technique (the Malvern 2600D system) measures spray SMDs nonintrusively. The results show persistently that the spray droplet SMDs of the CWS containing smaller coal particles are larger than the SMDs of the CWS containing larger coal particles. This finding is consistent with the fact that the former exhibits larger viscosity than the latter. In addition, the internal capillary holding force between the particles and water increases with decreasing particle sues because of their smaller radii of curvature and larger total surface area. The increased holding forces of smaller coal particles enhance their resistance against the external airbfast and make the atomization difficult. However, smaller spray SMDs of the CWS containing larger coal particles are attributed to both their lower viscosity and their lower capillary holding forces, and thereby weaker resistance against the external airblast.

INTRODUCTION

Coal-water slurry (CWS) atomization involves interactions among three different phases: solid (coal particles), liquid (water and additives), and gas (air or steam). Both interfacial and rheological properties play important roles in determining atomization characteristics of slurry fuels. Rheology measurements show that slurry viscosity generally increases with decreasing mean particle size [1]. When the suspended coal particles are dispersed with stabilizing additives, adsorption or solvation layers form on their surfaces and increase their effective volumes. This effective volume increase is particularly significant for smaller particles because of their larger total surface area. The increased effective volume is attributed to the increasing slurry viscosity with decreasing mean particle size.

The interfacial tension of a slurry mixture is higher than that of pure liquid (water) because of the increased surface areas of the suspended solid particles [2]. The increase from that of pure water will be more pronounced for slurry containing smaller particles because of the larger total surface area. The slurry atomization and its rheology properties are significantly dependent on the coal particle size. Despite its importance, no correlation between the particle size and slurry atomization characteristics has been published to date.

The U.S. Department of Energy (US-DOE) sponsored this work, under Contract DE-FG 22-94PC94120. The authors would like to express grateful acknowledgment to Dr. S. S. Kim of the US-DOE Pittsburgh Energy Technology Center for supervising the research project.

Tsai and Knell [3] examined the effect of particle size distribution on CWS atomization by comparing different CWS samples containing polydispetse coal particles of unimodal or bimodal distributions. Sprays containing bimodal coal particles produced larger mass median diameters (Mlvms) than sprays containing unimodal coal of approximately identical mean particle diameter. The packing density of the bimodal sample is higher than that of the unimodal sample and so is the volumetric coal loading. The study suggests that the tighter packing of the bimodal particles can generate larger spray MMDs because of their stronger coalescence. The exclusive effect of coal particle size on atomization has not been addressed.

Cronin, Sojka, and Lefebvre [4] studied atomization with two different CWS samples containing different coal loadings and different size distributions of different means and ranges. The spray SMD data showed some evidence that CWS containing smaller particles would produce larger spray droplets than CWS containing larger particles. However, since the coal loadings of the two samples were different, and each sample contained polydisperse coal particles of different distributions, their observation was not sufficient in determining the unique effect of particle size on slurry atomization.

This article presents a systematic investigation of the effect of particle size on atomization characteristics of CWS sprays containing classified coal particles in different size ranges. Both radial and axial SMD variations are presented for three different CWS samples containing coal particles of different sizes under airblast injection pressures ranging from 128.9 kPa (4 psig) to 376.9 kPa (40 psig).

EXPERIMENTS

Coal-Water Slurry (CWS) Sample Preparation

A batch of selected coal (Elkhorn Seam, Virginia: 60.7% fixed carbon, 36.7% volatile matter, and 2.6% ash content [5]) was classified into different size ranges using a sieve shaker. To minimize coal oxidation during sieving, the sieve array was sealed with tape and the duration of sieve shaking was kept at a minimum. Three samples (Figs. la-lc) were provided in the classified ranges of 32-45 μm, 45-63 μm, and 63-90 μm. All the tested CWS samples contained 40% weight coal loading. A rotating mixer, running approximately 12 h, completely mixed the coal and distilled/deionized water with the stabilizing additive of 0.5% Flown.

The photographs in Fig. 2 are coal particles sampled after being mixed with water. The sampling was made at the atomizing orifice and the water was dried from the sampled CWS. The long running time of the rotating mixer generated a significant amount of small crumbled particles. The disintegration is most severe for the sample containing the largest coal particles (63-90 Itm; Fig. 2c). The sample containing the smallest particles (32-45 μm; Fig. 2a) is nearly unchanged, since they are already as small as the crumbled particles. Despite the disintegration of larger particles in CWS mixing, the three samples are clearly distinguishable by their representative particle size ranges, which correspond generally to the original samples shown in Fies. la-lc.

Sonic Airblast Atomization System

Fig. 1 Classified coal samples in three different size ranges: (a) 23-45μm; (b)45-63μm; (c)63-90μm

exhausts from a mverging nozzle of 2.58 mm orifice diameter D_g for airblast atomization the cross-injected CWS mixture through 1.17 mm orifice diameter D_f. A positive-displacement syringe pumps the CWS mixture at a constant injection rate determined by

Fig. 2 Coal particles sampled from coal-water slurry mixtures of different size ranges: (a) 32-05 μm; (b) 45-. 63 μm; (c) 63-90 μm.

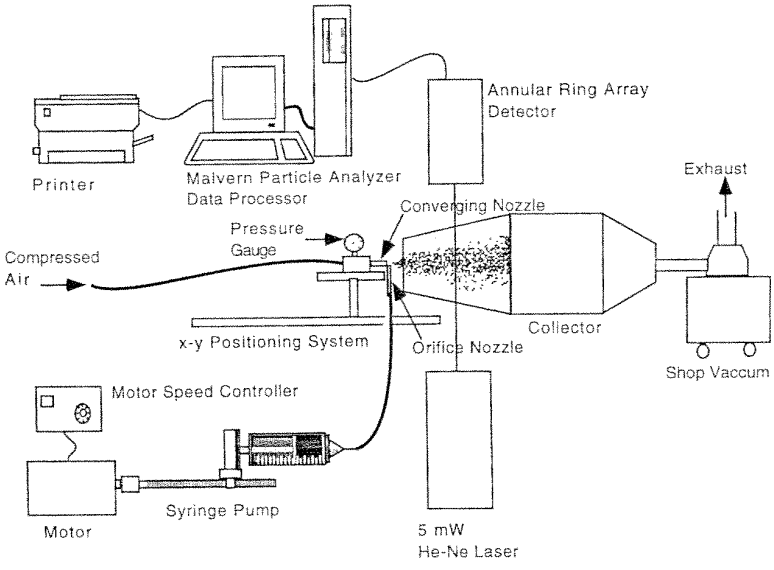

Fig. 3 Experimental setup of sonic airblast atomization system.

a stepper motor connected to a speed controller. The slurry injector needle is arranged perpendicular to the air nozzle and the injector exit is located near the nozzle center so that axisymmetric sprays develop. The spray symmetry has been examined by passing a flat sheet through the spray in parallel to the axis so that the streak patterns are recorded. Both horizontal and vertical streaks have approximately the same width, and this confirms the spray symmetry.

The Malvern diffraction particle analyzer [6] measures spray SMDs assuming RosinRammler [7] two-parameter distribution. The laser beam diameter of the Malvern system was reduced to 4.5 mm to improve the spatial resolution of SMD measurements [8]. Each spray SMD data point represents 600 sweeps of Malvern measurements. For selected data points, the batch of 600 sweep measurements was repeated several times and the measurement uncertainties were determined to be ± 7.85% on average.

The converging nozzle establishes a sonic exit flow when the stagnation pressure reaches 191.7 kPa (13.1 psig or 27.8 psia) for one atmospheric back pressure of 101.3 kPa (0 psig or 14.7 psia). This condition is called a perfect or isentropic expansion. When the stagnation pressure exceeds 191.7 kPa, the jet Mach number remains at unity, but the jet exit condition becomes an underexpanded state and exhausts an increased air mass flow. Thereafter, the air flow rate increases linearly with the stagnation pressure [9]. This increased mass flow rate of the underexpanded sonic jet enhances the airblast shear energy and generates very fine sprays [10].

Rheology Measurement

A rotating cylinder viscometer measured the CWS viscosity as a function of the shear rate. Figure 4 shows viscosity versus shear rate for the three CWS samples of different coal particle size ranges with the same coal loading of 40%. All three curves show gradual shear thinning and pseudoplastic behavior [1 lj, which is known as a consistent character of CWS mixtures. The CWS viscosity increases with decreasing coal particle sizes under the same coal loading. The increased number density and total surface area of smaller coal particles creates larger resistance to their relative motion in water.

As the viscosity measurement was possible only for the low-shear-rate range while the actual atomization occurs at higher shear rates by orders of magnitude, the reported viscosities may have little direct relevance to actual viscosities under atomization. However, the purpose of the reported viscosity measurement is to show that the CWS viscosity increases with decreasing coal particle sizes, not a full correlation of CWS viscosity versus shear rates. Since the viscosity is known to increase droplet sizes [12j, CWS containing smaller coal particles is expected to atomize into relatively larger droplets compared with CWS containing larger coal particles.

The atomization process creates new surfaces and drives coal particles to diffuse from the CWS bulk into the newly created surfaces. In order to characterize CWS surface properties, two separate measurements were made for both static and dynamic surface tension coefficients. Static surface tension was measured using a du Nouy ring tensiometer, allowing the sample to reach an equilibrium after the surface was expanded and all the coal particles were completely diffused along the expanded surface. Dynamic surface tension [13] was measured using a maximum bubble tensiometer (Fig. 5) before equilibrium was reached, while the coal particles were diffusing along the expanding surfaces. The measurements were repeated for CWS samples containing coal particles in different size ranges.

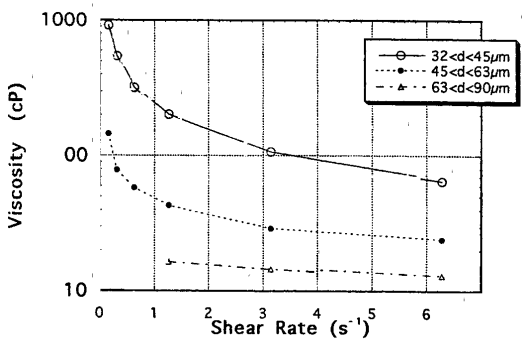

Fig. 4 CWS viscosity versus shear rate for the three tested samples.

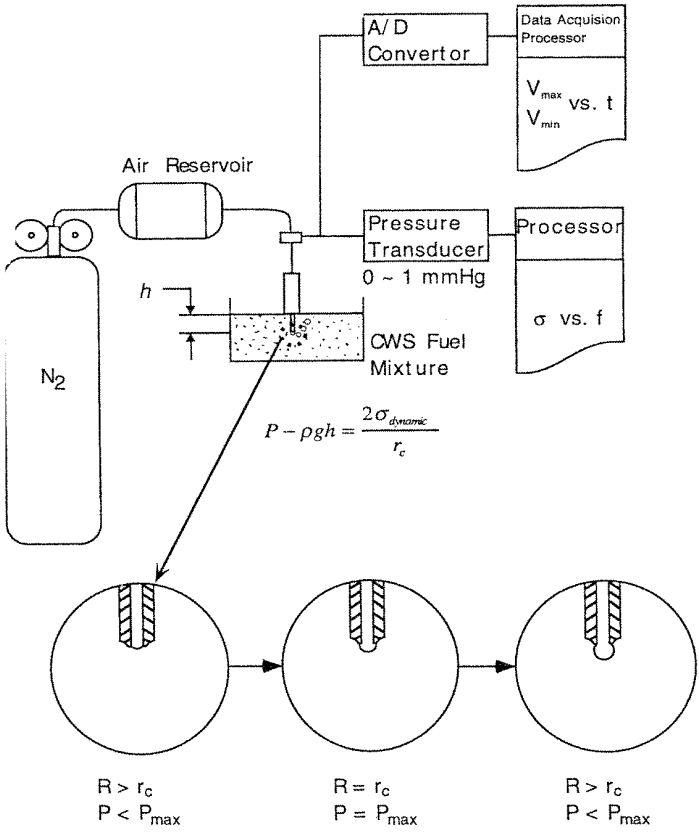

Fig. 5 Schematic illustration of a maximum bubble-pressure detection technique for dynamic surface tension measuremnet

Measured static surface tension values (Table 1), regardless of their particle size ranges, are approximately equal to the surface tension of pure water (72.5 dyne/cm at 20 °C) within the measurement uncertainties of approximately 3%. However, the CWS dynamic surface tension, measured at 10 Hz of bubble frequency, shows a persistent dependence on coal particle size ranges.

As illustrated in Fig. 5, a capillary tube with a small inside diameter (~1 mm) has its opening h below the free surface of the CWS sample. As bubbles form, grow, and detach from the capillary tube orifice, variations of the bubble pressure occur from the change in bubble radius. A maximum pressure is recorded for each bubble when the bubble radius reaches its minimum at the orifice radius. The dynamic surface tension for different bubble

Table 1 Static and Dynamic Surface Tension Data for Three Different CWS Samples Containing Coal Particles in Different Size Ranges [2].

	Coal particle size range		
	32 < d < 45 μm	45 < d < 63 μm	63 < d < 90 μm
Static surface tension (N/m)	0.0729	0.0726	0.0725
Dynamic surface tension (N/m)	0.0760	0.0750	0.0730

generation frequencies is then calculated from the measured maximum bubble pressure substituted into a simple relation:

$$\sigma = \frac{(p_{\max} - \rho g h) r_c}{2} \tag{1}$$

where ρ is the sample fluid (CWS) density, g is the gravitational acceleration, h is the depth of the capillary outlet, and r_c is the radius of the capillary outlet. The maximum bubble pressure, p_{max}, corresponds to the inside air pressure when the radius of the growing bubble equals the capillary radius, r_c.

Dynamic surface tension of a pure substance, such as water, should be identical to its static surface tension, since the molecular characteristic time for diffusion is very short. However, for CWS mixtures, where the coal particle characteristic time for diffusion is much slower, their dynamic surface tension values are consistently larger than their static surface tension values (Table 1). Although the dynamic surface tension data were only *5%* larger than their static counterparts, the measurement showed persistent increases. The large number density and increased total surface area of coal particles makes surface expansion more difficult and requires a longer time for the same amount of surface expansion.

RESULTS AND DISCUSSION

Figure 6 shows droplet SMDs measured along the spray axis x for CWS volume flow rate Qr = 2 ml/s under an underexpanded sonic airblast jet at *239* kPa *(20* psig). Spray SMDs first decrease because of the initial breakup of CWS ligaments into smaller droplets, and a minimum SMD is achieved at a certain x location. The spray SMDs then gradually increase, probably because of the coalescence between droplets as they travel downstream. In order to support the idea of coalescence, back-of-the-envelope calculations estimate the local droplet number density. For *20* psig condition, the volume flow rate of air jet after complete expansion to atmospheric pressure (near the location of minimum SMDs) is estimated to *2,250* ml/s assuming negligible jet entrainment. Thus, the local number density ranges from 1,700/ml to 1,700,000/ml for monodisperse droplet diameter ranging from 100 μm to 10 μm. Coalescence is most likely to occur in such dense sprays when sampled at large distance from the atomizer exit [14].

Preferential evaporation of smaller droplets also contributes to gradually increasing the spray SMDs

critical diameter of dried-off droplet, that is, $d^2_{crit=\lambda t}$, as approximately 7.0 μm. The calculation used the evaporation constant λ = 0.1 mm^2/s and the travel time of *0.5* ms to a location 10 cm downstream of the nozzle exit. This means that droplets below 7.0 gm diameter will be dried off before they reach the location of x = 10 cm and the average droplet SMD increases because of the dry-off of smaller droplets.

Another possible contribution to the gradual increase of SMDs is the well-known droplet size-velocity correlation, whereas the Malvern measures only the size correlation. Bigger droplets, because of their larger ratio of inertia to drag, travel more distance in a given time of flight than smaller droplets. Thus, after the minimum SMD location, smaller droplets are dispersed from the spray core to the spray boundary and the resulting spray SMDs can gradually increase.

The location of minimum SMDs, x_{min}, remains at approximately X_{min}/D_g = *40 (x = 10.3* cm and D_g = *2.58* mm) for all tested conditions of different stagnation pressures and different coal particle size ranges. Representative SMDs are measured at X_{min}/D_g = *40,* as recommended by the ASTM Standards on Liquid Particles and Sprays [15]. Note that the spray SMDs shown in Fig. 6 decrease with increasing coal particle sizes when other injection conditions are fixed. CWS viscosity decreases with increasing coal particle size ranges (Fig. *4).* These lowered physical properties make the breakup of CWS containing larger particles easier and produce smaller spray SMDs.

A more rigorous physical explanation for the slurry atomization characteristics considers capillary pressure and holding (coalescence) forces between suspended coal particles in water. Figure 7 illustrates the schematic of slurry breakup/atomization depending on their particle sizes. Upon injecting a CWS mixture, the sonic air jet at high pressure and velocity shatters the coagulated CWS bulk (ligaments) packed by capillary holding of coal particles. When particles are large, their larger radii of curvature give a

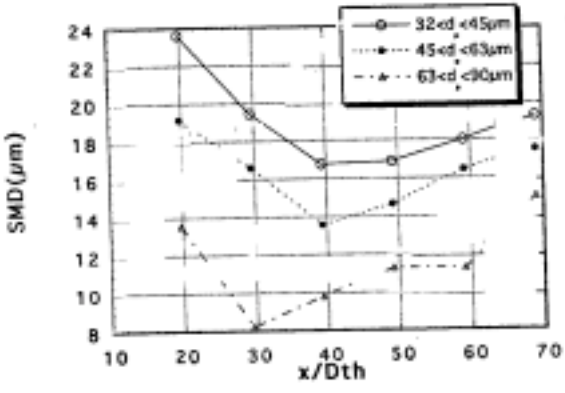

Fig. 6 Axial spray SMD variations for the three tested CWS under 40% weight loading.

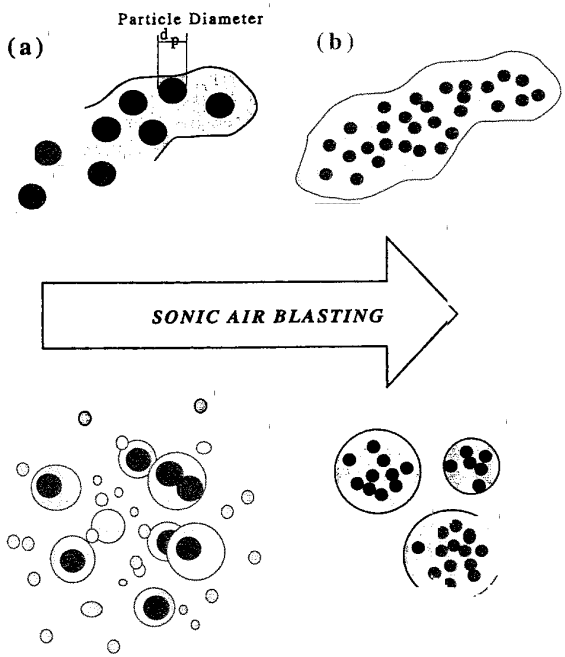

Fig. 7 Schematic illustration of atomization of two different slurry (ligaments) containing larger coal particles (a) and smaller coal particles (b).

weaker capillary holding force and loosely retain water between them. This weak hydration bonding allows large particles to separate easily from each other and from water when exposed to a strong, shattering air blast. The lower number density and smaller total surface area of larger particles also make their coalescence weaker. Therefore, atomizing a CWS mixture containing large coal particles consists of a twofold feature: (I) fine sprays of nearly pure water droplets generated from water separated from coal particles, and (2) droplets containing a limited number of large coal particles that are easily separated from the mixture.

For CWS containing smaller coal particles, the high particle number density and larger total particle surface area provides strong capillary bonding forces between the particles, as well as between particles and water. Water will not easily strip off the coal particles because of the strong hydration bonding, and the strong coalescence between particles will atomize each drop to contain many fine particles. This supports the physical explanation of why CWS containing smaller particles atomizes into a spray of a larger SMD.

Figure 8 shows more evidence of the above findings in terms of measured drop SMD spectra. Spray conditions are identical to those in Fig. 6. Measurements were made at the

axis location of minimum CWS spray SMDs, that is, $x_{min}/D_g = 40$ and y = 0, where y is radius. As the coal particle size increases, the CWS spray spectrum approaches the purewater spray spectrum. This shows that the spray may contain a significant portion of nearly pure water spray atomized from the readily separated water when particles are large. For CWS containing smaller particles, however, the spray drop size spectrum moves away from the pure water spectrum, showing a larger SMD. This supports that smaller coal particles coagulate more strongly and use a high capillary holding force to retain water between them. Both the strong packing and strong hold of water contribute to the relatively large SMDs for CWS containing smaller coal particles.

Figures 9a-9c show the CWS spray SMD variations in the radial direction at , $x_{min}/D_g = 40$ for the three tested samples all at 2 ml/s injection rate. The three air stagnant conditions of 10, 20, and 40 psig are equivalent to Weber numbers ($We \equiv \rho_g U_g^2 D_f/\sigma_f$) of 1655, 2757, and 4349, respectively. The air density at the air orifice exit, ρ_g, *is* 1.363 kg/m^3 (exit Mach number = 0.88; P_e, = 101.3 kPa, and T_e = 259 K), 1.760 kg/m^3 (underexpanded sonic exit; P_e = 126.3 kPa, and T_e = 250 K) or 2.776 kg/m^3 (underexpanded sonic exit; P_e = 199.2 kPa, and T_e =250 K). The air jet velocity, U_g, is taken equal to the orifice exit velocity, i.e., 279 m/s for 10 psig stagnation pressure, and 317 m/s for the choked exit thereafter. A median value for CWS dynamic surface tension coefficient is taken as σ_f = 0.075 N/m from Table 1. The air flow Reynolds numbers based on the orifice exit diameter ($\mathrm{Re} \equiv \equiv \rho_g U_g D_f / \mu_g$) are 5.9 x 10^4, 9.0 x 10^4, and 1.42 x 10^5, respectively, for the three stagnant pressure conditions, 10, 20, and 40 psig.

The spray SMDs increase with distance away from the spray center. This is attributed in part to preferential evaporation of fine droplets, as previously discussed with estimation based on sample calculations using d^2 law. The air jet diffuses rapidly and the jet quickly slows down near the spray boundary. This weakened airblasting shear energy reduces the atomization efficiency near the spray boundary and contributes to the larger spray SMDs there. Another important reason for larger SMDs for the region away from the centerline is likely because of the well-known size-dependent inertia-drag mechanism, the so-called

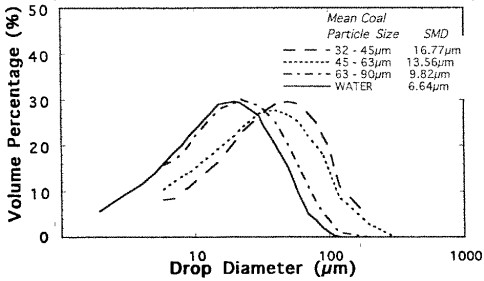

Fig. 8 Volumetric percentile spectra of droplets of the three tested CWS sprays and water spray at 239.1 kPa (20 psig) air jet pressure.

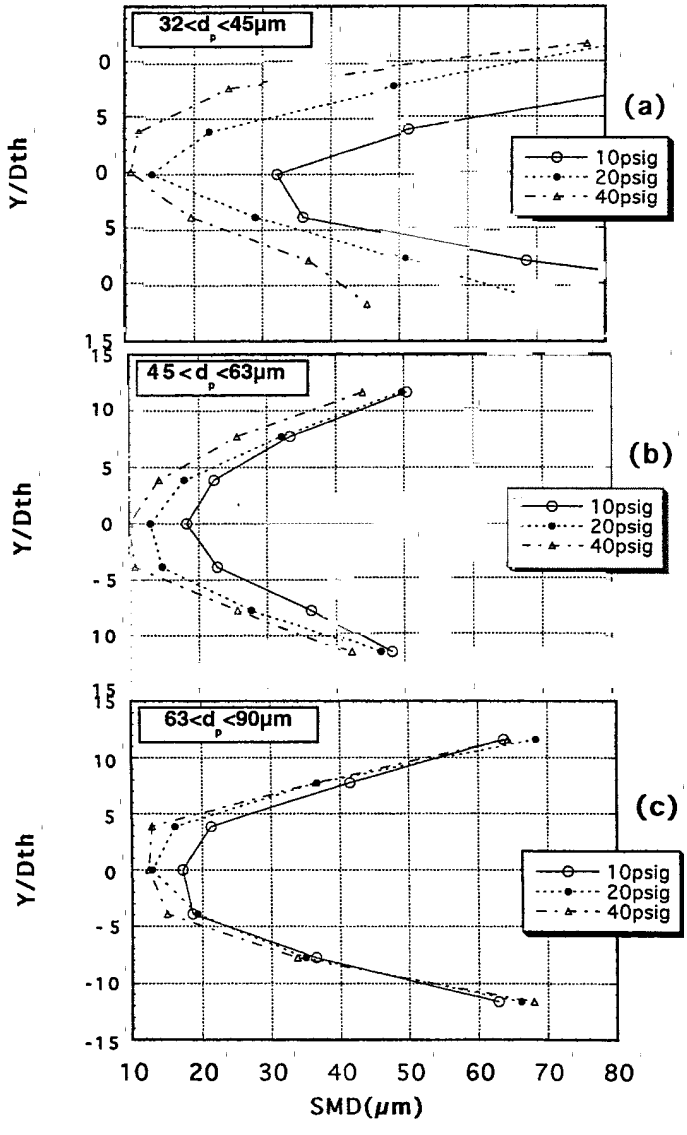

Fig. 9 Radial SMD variations of 40% CWS sprays at $x/D_{th} = 40$ under different air jet pressures: (a) 32 μm < d_P < 45 32 μm; (b) 45 32 μm < d_p < 63 32 μm; (c) 63 32 μm < d_P < *90* 32 μm

droplet size-velocity correlation. The high ratios of drag to inertia of small droplets allow them to easily ride with the high-speed air flow along the spray axis. On the other hand, larger droplets, because of their large inertia, tend to disperse away from the center and slow down into the spray boundary region. As a result of this, the spray center region measures smaller SMDs.

The spray SMDs decrease with increasing air jet pressure for each CWS sample. A sudden decrease in SMD distribution occurs when the external action of the high-pressure airblast overrides the internal resistance of capillary holding, as shown in Fig. 9a by the large SMD reduction from 170 to 239 kPa (10 to 20 psig, respectively).

The transition in spray SMDs is more pronounced for the CWS containing the smallest particles (Fig. 9a), but the dependence gradually decreases with increasing particle size (Figs. 9b and 9c). When particles are small (Fig. 9a), the capillary holding is so strong that the airblast at 10 psig is not enough to initiate the transition to the breakup of capillary holding. The resulting spray SMDs are relatively large. The stronger airblast jets at 239 and 377 kPa (20 and 40 psig, respectively) enable the spray to pass the transition and significantly reduce the spray SMDs. When particles are larger (Fig. 9b), the relatively weak capillary holding can be readily shattered at lower jet pressures (possibly lower than 239 kPa or 20 psig), and the spray transition occurs at all three levels of jet pressure. The SMD dependence on the jet pressure nearly disappears for CWS containing the largest coal particles (Fig. 9c), where the spray transition to the dominant airblast over capillary holding is prevalent for all three pressure levels.

Figures l0a-10d show the effect of air jet pressure and the effect of particle size range on slurry atomization. For the jet at 129 ki?a or 4 psig (Fig. 10a; $We = 797$, $Re = 3.7 \times 10^4$, and nozzle exit velocity of air $U_g = 201$ m/s or $M = 0.60$), the aforementioned transition, i.e., airblast domination over the capillary holding, occurs only for the CWS spray containing the largest coal particles with the weakest capillary holding among the three. This transition shifts toward CWS sprays containing smaller coal particles as the jet pressure increases. The transition occurs with the medium sample ($45 < d_P < 63\ \mu m$) at 170 kPa (10 psig) jet pressure (Fig. 10b) and eventually with all three samples at 239 kl?a or 20 psig (Fig. 10c). All three SMD curves nearly collapse into a single curve at 377 kPa or 40 psig. This indicates that the internal capillary holding is sufficiently dominated by the strong airblast, regardless of particle size range, that no apparent effect of particle size on atomization is shown.

Figure 11 shows spatially averaged SMDs after tomographic reconstruction of the line-of-sight Malvern data presented in Fig. 10. Axisymmettic sprays are assumed to have concentric ring regions of different SMDs and the use of Abel inversion [16, 17] of the line-of-sight Malvern data provides a reconstructed radial SMD distribution. The radial SMD of each concentric region then has been multiplied by its concentric area (A_i) and volume concentration (C_i), and the summation of all weighted SMDs is divided by the summation of A_i and C_i to calculate the spatially averaged SMD, i.e.,

$$\overline{SMD} = \frac{\sum_{i=1}^{N} SMD_i \cdot A_i \cdot C_i}{\sum_{i=1}^{N} A_i \cdot C_i} \qquad (2)$$

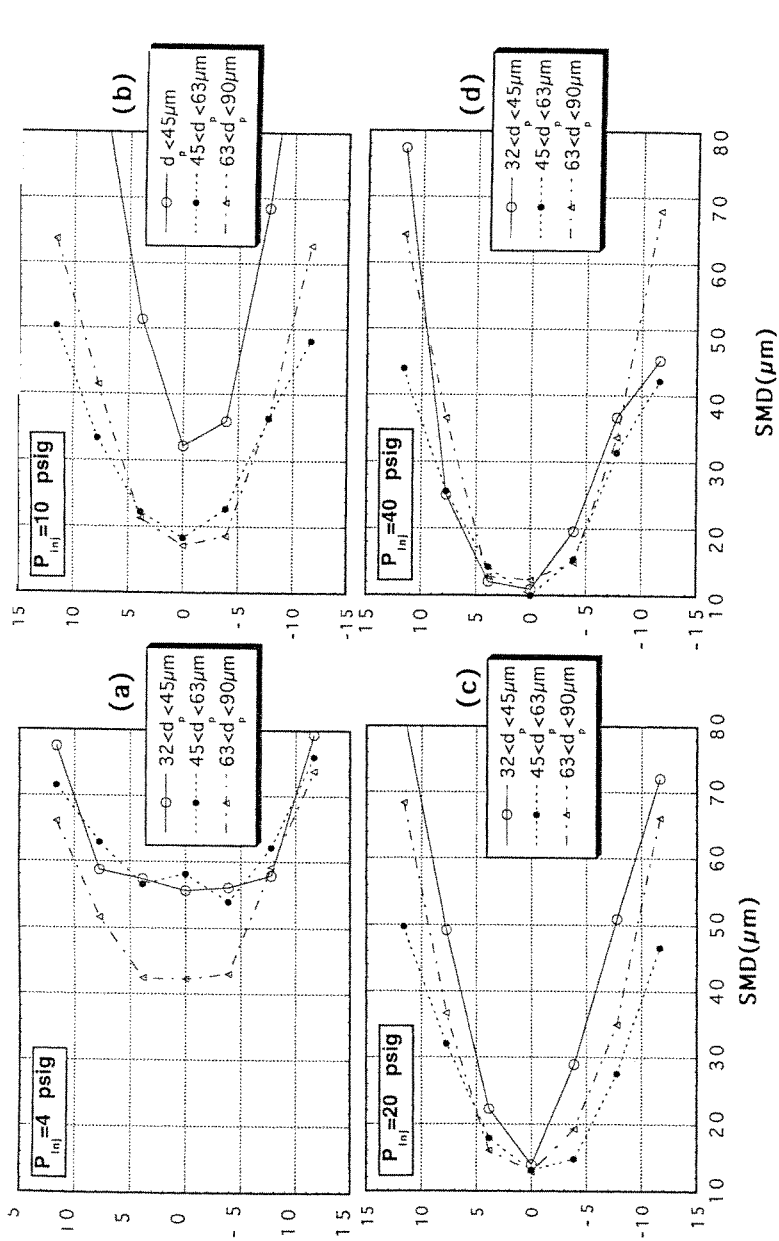

Fig. 10 Radial SMD variations of the tested three different CWS sprays measured at $x/D_{th} = 40$: (a) air jet pressure $P_{inj} = 129$ kPa (4 psig); (b) 170 kPa (10 psig); (c) 239 kPa (20 psig); (d) 377 kPa (40 psig).

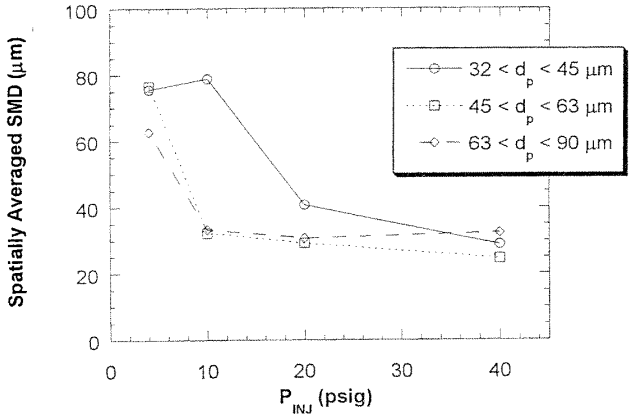

Fig. 11 Tomographically reconstructed and spatially averaged SMDs versus injection pressure for three CWS mixtures.

The spatially averaged SMDs show a significant decrease at a certain threshold gas injection pressure for each of the three CWS mixtures. As discussed previously, this threshold occurs when the external inertial force overrides the internal holding force and a significant improvement in atomization is expected. The slurry mixture containing smaller particles ($32 < d_p < 45$ μm) requires the highest threshold gas injection pressure because of their largest capillary holding. All three sprays beyond 20 psig have exceeded their threshold pressures and their SMDs merge, indicating a weaker effect of particle size on atomization.

CONCLUSION

Slurry atomization is a process that by airblast drives the *transition* from the tightly packed particle/water bulk under strong capillary holding forces into atomized spray droplets. For CWS containing larger coal particles, the transition occurs at a relatively lower airblast jet pressure. The transition for CWS containing smaller particles is delayed until the jet pressure reaches a higher level. This dependence of the slurry spray transition on the particle size range explains why CWS containing larger coal particles generates finer sprays and CWS containing smaller coal particles generates a spray of a larger mean diameter.

The CWS containing large particles holds water loosely because of its weak capillary holding forces. This makes coal particles separate easily between themselves as well as between particles and the water. The resulting spray con sists of both nearly

pure water droplets of very small diameters generated from the water stripped from the mixture, and of smaller CWS droplets containing a limited number of coal particles. Consequently, the overall mean drop diameter shows a decrease with increasing coal particle size. On the other hand, smaller coal particles strongly coalesce to one another and strongly retain water between them. This enables their CWS mixture to atomize into larger drops that still contain a number of tightly packed coal particles. The high capillary holding and tight packing is attributed to larger SMDs of CWS sprays containing smaller particles.

Concurrently, the effect of viscosity plays an important role in CWS atomization. The viscosity is known to increase droplet sizes. Theoretical study of liquid breakup mechanism by Lin and Lian [12] shows that an increase of viscosity by 22 times results in an increase of 30% in the most probable drop size for the case of liquid jet breakup. The present experimental study shows that the measured SMD increases less than 100% from CWS containing coal particles in $63 < d < 90$ μm to CWS containing coal particles $32 < d < 45$ μm as the apparent viscosity is increased by more than 10-fold (Fig. 4). These results are consistent in order of magnitude with the known theoretical results on the effect of viscosity.

REFERENCES

1. G. D. Botsaris and Y. M. Glazman, *Interfacial Phenomena in Coal Technology,* Chap. 3, Marcel Dekker, New York, NY, 1989.
2. K. D. Kihm, Effect of Coal Particle Sizes on the Interfacial Properties of Coal-Water Slurry (CWS) and Its Atomization Characteristics, US-DOE Contract DE-FG 22-94PC94120 Final Report, 1996.
3. S. C. Tsai and E. W. Knell, Rheology and Its Effects on Atomization of Coal Water Slurry,*Proc. First Annual Pittsburgh Coal Conf, pp.* 190-200, 1984.
4. L. Cronin, P. E. Sojka, and A. H. Lefebvre, The Effect of Fuel Film Thickness on Coal Water Slurry Atomization, SAE Paper 852086, 1985.
5. K. D. Kihm, Development and Use of an Apparatus to Measure the Dynamic Surface Properties of Coal-Water Slurry Fuels for Applications to Atomization Characteristics, US-DOE Contract DE-FG 22-92PC92156 Final Report, 1994.
6. H. G. Barth, *Modern Methods of Particle Size Analysis,* Chap. 5, John Wiley, New York.NY, 1984.
7. R. Rosin and E. Rammler, The Laws Governing the Fitness of Powdered Coal, *Institute of Fuel, pp.* 29-36, 1933.
8. K. D. Kihm and J. A. Caton, Synchronization of a Laser Fraunhofer Diffraction Drop Sizing Technique with Intermittent Spray Systems, *Appl. Opt., vol.* 31, no. 12, pp. 1914-1916, 1992.
9. J. E. A. Jones, *Gas Dynamics,* 2nd ed, Chap. 3, Allyn & Bacon, Boston, MA, 1984.
10. B. K. Park, J. S. Lee, and K. D. Kihm, Comparative Study of Twin-Fluid Atomization Using Sonic or Supersonic Gas Jets, *Atomization and Sprays,* vol. 6, pp. 285-304, 1996.
11. R. J. Hunter, *Foundation of Colloid Science, vol. I,* pp. 87-89, Clarendon Press, Oxford, UK, 1986.
12. S. P. Lin and Z. W. Lian, Mechanism of the Breakup of Liquid Jets, *AIAA J.,* vol. 28, pp. 120-126, 1990.
13. K. D. Kihm and P. Deignan, Dynamic Surface Tension of Coal-Water Slurry Fuels, *Fuel, vol.*74, pp. 295-300, 1995.
14. A. H. Lefebvre, *Atomization and Sprays,* Hemisphere, New York, NY, 1989.

15. ISBN 0-8031-1762-0, *ASTM Standards on Liquid Particles and Sprays,* E-1260, pp. 8-11, ASTM Press, Philadelphia, PA, 1992.
16. D. C. Hammond, Jr., Deconvolution Technique for Line-of-Sight Optical Scattering Measurements in Axisymmetric Sprays, *Appl. Opt., vol.* 20, pp. 493-499, 1981.
17. L. G. Dodge, D. B. Rhodes, and R. D. Reitz, Drop-Size Measurement Techniques for Sprays: Comparison of Malvern Laser-Diffraction and Aerometrics Phase/Doppler, *Appl. Opt., vol.* 26, no. 11, pp. 2144-2154, 1987.